Journal of Physiology (1991), **441**, *pp.* 685–702
With 8 figures
Printed in Great Britain

KINETICS OF ADENOSINE TRIPHOSPHATE HYDROLYSIS BY SHORTENING MYOFIBRILS FROM RABBIT PSOAS MUSCLE

BY T. OHNO* AND T. KODAMA†

*From the *Department of Physiology, Jikei University School of Medicine, Tokyo 105, Japan and the †Department of Biochemistry, Okayama University Dental School, Okayama 700, Japan*

(*Received 5 February 1990*)

SUMMARY

1. Using a solenoid-operated mixing device, time-resolved measurements were made of shortening and accompanying ATP hydrolysis at 20 °C by myofibrils prepared from rabbit psoas muscle.

2. The extent of ATP hydrolysis was determined by an improved Malachite Green method for determination of inorganic phosphate (P_i) in the presence of a large excess of ATP. For the measurement of the change in sarcomere length by phase contrast microscopy, shortening was terminated without delay and artifact by a mixture of 0·2 M-acetate (pH 4·6) and 1·25% (v/v) glutaraldehyde.

3. The shortening velocity per half-sarcomere was 10 μm s^{-1} in 25 mM-KCl for sarcomere lengths above 1·4 μm, and at least 12 μm s^{-1} in 150 mM-KCl for sarcomere lengths above 1·7 μm. During this rapid shortening, there was no significant ATP turnover by cross-bridges (upper 95% confidence limit: 0·14 mol (mol of myosin head)$^{-1}$ in 25 mM-KCl; 0·12 mol mol^{-1} in KCl solutions $\geqslant$ 100 mM).

4. When the sarcomeres shortened below 1·7 μm in KCl concentrations > 100 mM or below 1·4 μm in 25 mM-KCl, there was a transient acceleration of ATP hydrolysis (delayed ATP hydrolysis), which was then followed by a steady slow hydrolysis.

5. The magnitudes ($\pm$estimated standard deviation) of delayed ATP hydrolysis by myofibrils of initial sarcomere length 2·4 μm were 0·42$\pm$0·19, 0·31$\pm$0·10 and 0·17$\pm$0·09 mol (mol myosin head)$^{-1}$ in 25 mM, 100 mM and 150 mM-KCl, respectively. For myofibrils of sarcomere length 2·0 μm, however, it decreased to 0·24$\pm$0·10 mol mol^{-1} in 25 mM-KCl or to an insignificant level in 150 mM-KCl.

6. These results indicate that most of the ATP hydrolysis products remain bound to cross-bridges during rapid shortening, and that when the force opposing shortening increases, a proportion of cross-bridges rapidly dissociate the products and enter the next ATP cycle, which diminishes with the decrease in shortening distance as well as the increase in ionic strength. Such behaviour of the cross-bridge is probably a manifestation of its energetic and kinetic properties in the state with bound ADP and P_i interacting with actin filaments at zero load and at a transition from zero to non-zero loads.

MS 8251

INTRODUCTION

Of several unsolved problems in muscle energetics (see Woledge, Curtin & Homsher, 1985; Homsher, 1987 for recent reviews), the 'unexplained' energy production by rapidly shortening muscle at or near the maximum velocities of shortening is most challenging. Heat is rapidly produced but the net turnover of ATP is very low during rapid shortening. This energy imbalance is compensated after the shortening by delayed ATP hydrolysis without heat production (Rall, Homsher, Wallner & Mommaerts, 1976; Homsher, Irving & Wallner, 1981). Such behaviour is in striking contrast to slower shortening and isometric contraction during which the ATP hydrolysis and total energy output (heat + work) are in phase and balanced after an initial period of imbalance (Homsher, Yamada, Wallner & Tsai, 1984). To pursue this problem in muscle energetics at the molecular level, one must know the ATP turnover rate during and after the rapid shortening. Currently available information is of insufficient accuracy or temporal resolution to examine the relation between chemical and energetic states of cross-bridges. This is because there are limitations for kinetic studies of ATP hydrolysis in whole muscle arising from technical difficulties of measurement and the presence of creatine phosphotransferase reaction and non-actomyosin ATP hydrolysis (see Homsher, 1987).

We used myofibrils prepared from rabbit psoas muscle in the work described here. Although myofibrils provide some advantages for kinetic studies (e.g. the rapid diffusion of the substrate), they are difficult to control mechanically. Nonetheless, it is likely that myofibrils shorten through at least two consecutive phases with different mechanical constraints, (1) shortening to sarcomere length of 1·6 μm and (2) shortening below that length. Thus, the strain imposed on the contractile apparatus is negligible (zero-load) in the first phase whereas the second phase is associated with an increasingly large strain (Gordon, Huxley & Julian, 1966; Edman, 1979; Allen & Moss, 1987). We have prepared myofibrils with a homogeneous sarcomere length for each experiment, and devised methods suitable for studying the time course of ATP hydrolysis during different phases of myofibril shortening. Our experiments indicate that: (1) the net turnover of ATP is almost negligible during rapid myofibrillar shortening; (2) after rapid shortening ceases, there is a transient burst of ATP hydrolysis (delayed ATP hydrolysis) followed by a steady rate of hydrolysis; and (3) the magnitude of the delayed ATP hydrolysis decreases with a decrease in shortening distance as well as an increase in ionic strength.

Preliminary results of these studies were presented at the Third International Conference on Muscle Energetics held in Japan, 1988 (Ohno & Kodama, 1989).

METHODS

Chemicals

ATP (code 519979 Boehringer Mannheim, Mannheim, Germany), was used without further purification (the level of inorganic phosphate (P_i) < 1·0 μM in mM solution). The Malachite Green (MG) reagent was prepared by adding 5·3 g sodium molybdate and 13 ml of 35% (w/w) HCl to 500 ml of a MG solution commercially available for P_i determination of clinical samples (Iatron Lab., Tokyo, see Kodama, Fukui & Kometani, 1986). The resultant mixture, containing 12·3 g sodium molybdate, 0·3 g MG and 0·5 g Sterox SE (polyethyleneglycol mono-*p*-nonylphenyl ether,

Monsant, St Louis, MS, USA) in 1 l of 1·0 M-HCl, was filtered through a sintered-glass filter and stored in a refrigerator. For daily use, this stock solution was diluted with an equal volume of 0·3 M-perchloric acid (diluted MG reagent). All the other chemicals were of reagent grade.

Myofibrils

Male rabbits weighing between 2·5 and 3·0 kg were stunned and killed by bleeding; the psoas muscles were dissected immediately and trimmed to make full-length strips of white muscle about 1 cm in width. Muscle strips were tied at rest length (for non-stretched myofibrils) or at 120–130% of rest length (for stretched myofibrils) to rigid bamboo sticks using thick (2 count) cotton thread. These strips were wrapped with poly(vinylidene chloride) film (Saranwrap, Asahi Chemical Ind., Tokyo), which prevents evaporation of wrapped material and penetration of air owing to its low permeability to gases (Yasuda & Stannett, 1975), and left overnight in a refrigerator to bring about rigor. All subsequent preparative steps were performed at temperatures below 4 °C. To prepare the fibrils with homogeneous sarcomere length, only the central 2 cm (*ca* 1 g in wet weight) of each strip was finely chopped and homogenized with a Waring blender in 20 ml of buffer containing 25 mM-KCl, 20 mM-3-(*N*-morpholino) propane sulphonic acid (MOPS)/KOH (pH 7·2) and 1 mM-EGTA. Homogenization was continued at top speed until (usually for 5 min without interruption) the suspension was found by inspection in a light microscope to contain mostly single myofibrils. Myofibrils thus prepared were washed three times with 10 volumes of the same buffer by centrifugation (900 *g* for 5 min), and finally obtained as a slurry containing 30–40 mg protein ml^{-1}. To prepare pre-contracted myofibrils, the muscles were homogenized within 1 h of the animals being killed. All myofibril preparations were used within 4 h.

ATP hydrolysis

A solenoid-operated rapid-mixing device was constructed according to Kanazawa, Saito & Tonomura (1970). For each measurement, a disposable polythene cup (inner diameter, 1·5 cm; height, 4 cm) was placed in the well of the device kept at 20 °C by circulating water from a constant-temperature bath. The solution in the vessel was continuously stirred by a Teflon-coated magnetic bar (diameter, 6 mm; length, 14 mm) rotating at 500 r.p.m. Additions were made from pre-loaded injectors actuated by solenoids that were controlled by pre-set relay timers. The reaction medium consisted of myofibrils (protein concentration, 1·5 mg ml^{-1}), 25–150 mM-KCl, 20 mM-MOPS/KOH (pH 7·2), 1 mM-$MgCl_2$, and either 1 mM-EGTA (for ATP hydrolysis in the absence of calcium ions) or 50 μM-EGTA (for Ca^{2+}-triggered experiments) in a total volume of 1·15 ml. In ATP-triggered experiments, EGTA was replaced by 0·5 mM-$CaCl_2$. The reaction was started by adding 50 μl of 50 mM-Mg-ATP (pH was adjusted to 7·2 with KOH) and quenched at different times with 1·0 ml of ice-chilled 0·67 M-perchloric acid (PCA). The acid-quenched reaction mixtures were centrifuged at 4 °C (1500 *g*, 1 min), and 2 ml of the diluted MG reagent pre-warmed to 25 °C was added to 0·2 ml of the supernatant. Since ATP hydrolysis was not negligible in PCA even at 0 °C (apparent first-order rate constant, 0·0015 h^{-1}), the period between acid-quenching and addition of the MG reagent was made constant (*ca* 90 min) for all samples. After vigorous shaking for 10–15 s, 0·2 ml 34% (w/v) sodium citrate (Lanzetta, Alvarez, Reinach & Candia, 1979) was added. After incubation for exactly 12 min at 25 °C, absorbance was measured at 650 nm. The extent of ATP hydrolysis was expressed as the ratio of mol P_i formed to mol myosin heads (cross-bridges) in the myofibrils by assuming that the molecular weight of myosin is 5×10^5, and that myosin occupies 43% of the total myofibril protein mass (Yates & Greaser, 1983). Protein concentration was determined by the biuret reaction (Gornall, Bardwill & David, 1949) with bovine serum albumin as standard.

Measurement of myofibril shortening

The reaction was started in the same way as in the ATP hydrolysis, but it was quenched with an equal volume of 0·4 M-sodium acetate buffer (pH 4·6) containing 2·5% (v/v) glutaraldehyde instead of PCA, and examined under a phase-contrast microscopy (Olympus BH-2) using an ocular with a built-in micrometer (Olympus OMS-4). For each sample, the sarcomere length is the mean value of those for thirty different myofibril fragments, each of which was estimated from the length of a straight part of a fragment consisting of at least five consecutive sarcomeres.

Presentation of data and statistics

The data points in figures are given with error bars showing ± one standard error of the mean (S.E.M.) unless the bars were too small to be illustrated. Student's t tests for significance and linear regression analysis were applied where required. To calculate the number of degrees of freedom (d.f.) associated with the differences between two values for which the variances (v_1, v_2) and the number of observations (n_1, n_2) were not equal ($v_1 \neq v_2$; $n_1 \neq n_2$), the following formula (Aspin, 1949) was used:

$$\text{d.f.} = 1/[k^2/f_1 + (1-k^2)/f_2],$$

where f_1 and f_2 are degrees of freedom of v_1 and v_2 respectively and k is defined by

$$k = (v_1/n_1)/(v_1/n_1 + v_2/n_2).$$

The value of k is to make due allowance for the relative magnitudes of the two variances. Thus, in calculations of the d.f. of a delayed ATP hydrolysis value (Table 3), the difference between estimated ATP hydrolysis calculated from the regression and observed ATP hydrolysis value (the mean of n_o observations), the formula for k can be written

$$k = v_e/(v_e + v_o/n_o),$$

where v_e is the variance of the estimated value and v_o is the variance of the observed value.

RESULTS

Evaluation of time resolution

We first tested the mixing efficiency of the solenoid-operated device. It was not feasible to observe the time course of mixing by fitting the device into the spectrophotometric instruments in our laboratory. We used an FET-pH sensor (Kraray, Okayama), which has a response time < 5 ms (Nakatuka, Nakamura & Sano, 1988). The time course of the pH change after adding 50 μl of 200 mM-HCl to 1·15 ml of the reaction medium (the HCl was a dummy of Mg-ATP in the myofibril experiments) is shown in Fig. 1*A*. The drop of pH to 7·05, which was expected to occur on mixing 10% of the total acid added, was completed within 10 ms, and 60% mixing (pH drop to 6·70) was completed by 20 ms.

Since the total added Mg-ATP was 2 mM in the present work, the substrate concentration must have been raised to > 1 mM in 20 ms, which was a more than fivefold excess over the myosin head concentration of 0·2 mM in myofibril lattice space (Yates & Greaser, 1983). Hence, pseudo-first-order conditions would have been achieved by 20 ms (see Ferenczi, Homsher & Tretham, 1984).

In Ca^{2+}-triggered experiments (see below), 0·5 mM-$CaCl_2$ was added to myofibrils relaxed with 2 mM-Mg-ATP in the presence of 50 μM-EGTA so that the free Ca^{2+} concentration must have been raised above 10^{-5} M within 10 ms. Thus, the rapid rise of ATP or Ca^{2+} concentration required in the present analysis were ensured under the conditions we used.

Quenching of ATP hydrolysis and shortening

Figure 2 shows that at pH's below 5, the ATPase rate of myofibrils was < 10% of that at neutral pH. When 1·0 ml of 0·67 M-perchloric acid (PCA) was added to 1·2 ml of the reaction medium, the pH fell below 4·5 within 10 ms (Fig. 1*B*). It is consistent with these observations that no ATP hydrolysis occurred when PCA was added to myofibrils simultaneously with ATP. These results indicate that there was little delay (< 10 ms) in termination of ATP hydrolysis.

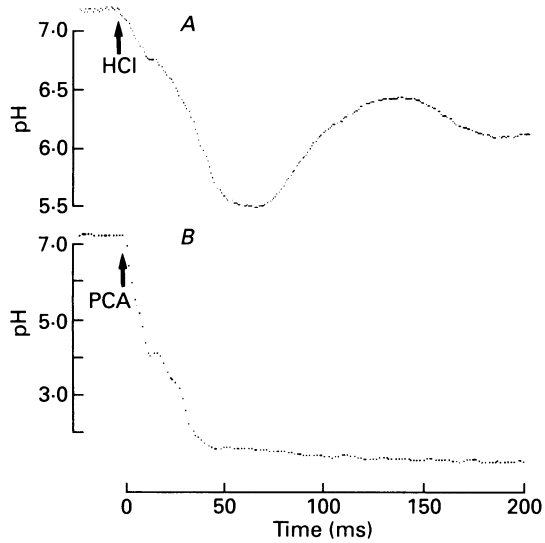

Fig. 1. Test of mixing efficiency of the solenoid-operated mixing device. The FET pH sensor ($5{\cdot}50 \times 0{\cdot}40 \times 0{\cdot}15$ mm^3) with a flexible, thin lead (1 mm in diameter) was immersed in the buffered salt solution of the same composition as for myofibril experiments; the output of the sensor (58 mV (pH unit)$^{-1}$) was monitored by a digital oscilloscope triggered on injection of acid. Data from ten measurements were treated by averaging and digital filtering. Additions: *A*, 50 μl of 200 mM-HCl; *B*, 1 ml of 0·67 M-perchloric acid (PCA).

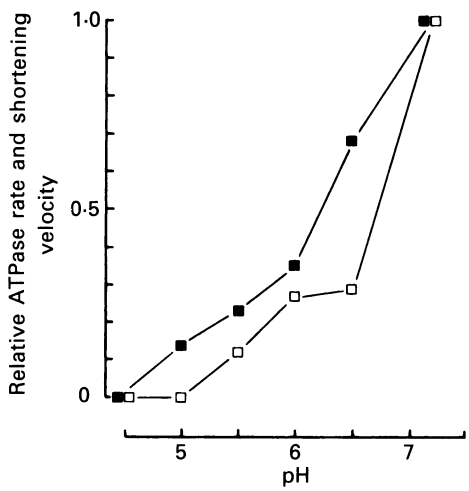

Fig. 2. Effects of pH on myofibrillar ATPase rate (■) and shortening velocity (□). A preparation of stretched myofibrils (sarcomere length, 2·5 μm) was used in the reaction medium containing 25 mM-KCl; pH was adjusted by adding appropriate amounts of 0·2 M-acetic acid. Both ATPase rate and shortening velocity are relative to those at pH 7·2 (3·2 s^{-1} and 10·1 μm s^{-1} (half-sarcomere, h.s.)$^{-1}$, respectively). See Figs 4 and 7 and text for experimental details.

Shortening of myofibrils also slowed sharply when the pH was lowered and became negligible at pH's below 5·0 (Fig. 2). Hence, sudden lowering of the medium pH to below 5·0 was expected to halt shortening rapidly. A fall of pH in < 10 ms was attained by mixing the reaction medium with an equal volume of 0·4 M-acetate (pH 4·6) in the rapid mixing device (data not shown). Myofibrils did not shorten,

TABLE 1. Effects of acetate and glutaraldehyde mixture on sarcomere length

Myofibril preparation		Length (μm) Before	After
A	Sarcomere	2·85±0·08 (30)	2·83±0·08 (30)
	I-band	1·32±0·11 (28)	1·36±0·10 (29)
	A-band	1·53±0·13 (23)	1·46±0·12 (24)
B	Sarcomere	2·01±0·06 (29)	1·98±0·07 (28)
C	Sarcomere	2·03±0·10 (30)	1·99±0·05 (29)

Length was measured before and after addition of acetate and glutaraldehyde.
Myofibril preparation A was obtained from the muscle strip stretched to 140% of rest length. Preparations B and C were non-stretched myofibrils; the latter was first mixed with 2 mM-Mg-ATP in the presence of 1 mM-EGTA in 150 mM-KCl and then with the acetate and glutaraldehyde mixture. Data in the table are means±S.D. for numbers of observations in parentheses. Note that no preparation showed variation in sarcomere length greater than 0·1 μm. The length of the A-band is not significantly different from the values given by Hanson & Huxley (1955) and Page & Huxley (1963).

when mixed with acetate and ATP simultaneously. Thus, although acetate alone was effective at preventing myofibril shortening, it was supplemented with glutaraldehyde to assure that no shortening would occur during storage after quenching or during microscopic observation.

Table 1 shows that the acetate–glutaraldehyde mixture did not cause any significant change in sarcomere length irrespective of the initial length. A-band or I-band length did not change either. Furthermore, when myofibrils were first relaxed by mixing with 2 mM-Mg-ATP in the presence of 1 mM-EGTA in 150 mM-KCl (see next section) and then quenched with the mixture, no significant effect on sarcomere length was observed (preparation C). These results are consistent with the observation by Page & Huxley (1963) that glutaraldehyde causes very little shortening of both the thin and thick filaments. Thus, the acetate–glutaraldehyde mixture proved to be a reliable quencher of myofibril shortening without appreciable delay (< 10 ms) and artifact.

Shortening of myofibrils

Shortening in the absence of calcium ions

In the medium containing 25 mM-KCl and 1 mM-EGTA, there was a slow shortening of myofibrils on addition of ATP for the first 100–200 ms, which became progressively slower. This time course of shortening was somewhat variable from one preparation to another (Fig. 3). Much the same results were obtained in 50 and 75 mM-KCl.

When KCl concentration was higher than 100 mM, on the other hand, no significant shortening took place on addition of ATP, provided the sarcomere length

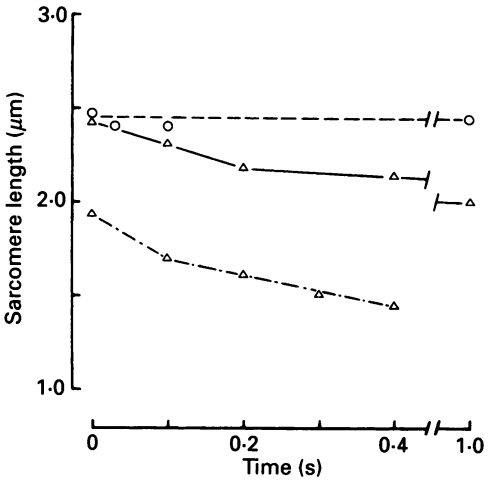

Fig. 3. Changes in sarcomere length of myofibrils induced by Mg-ATP (2 mM) at time = 0 in the absence of calcium ions. EGTA (1 mM) was added to myofibril suspensions before addition of ATP. Symbols: △, 25 mM-KCl; ○, 150 mM-KCl. Error bars of ± 1 S.E.M. are too small to be illustrated.

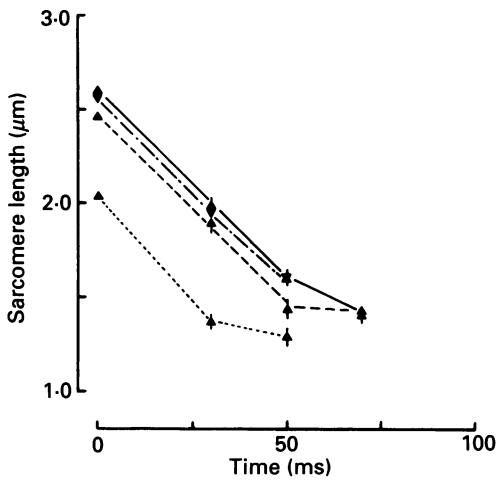

Fig. 4. Active shortening of myofibrils in the medium containing KCl concentrations below 100 mM. Mg-ATP (2 mM) was added at time = 0 to the medium containing 0·5 mM-$CaCl_2$. Symbols: ▲, 25 mM-KCl; ▼, 50 mM-KCl. Error bars represent ± 1 S.E.M.

was not greater than 2·7 μm. From this result, we can exclude any contribution from the passive compressive force by the parallel elastic component to the rapid shortening of myofibrils induced by ATP described below.

Active shortening

Active shortening was triggered by ATP in the presence of 0·5 mM-added $CaCl_2$ at low ionic strengths (KCl < 50 mM) (Fig. 4). Stretched myofibrils (initial sarcomere length, 2·4–2·6 μm) rapidly shortened almost linearly over a distance of 1·0 μm for

the first 50 ms. In the following 50 ms, the shortening slowed, and contraction bands gradually appeared. At 150 ms and thereafter, amorphous aggregates were the dominant features of the myofibril structure.

A similar rapid shortening was observed for non-stretched myofibrils for the first 30 ms. The majority of these myofibrils, however, already showed intense contraction bands at 50 ms, and some changed into amorphous aggregates even at 100 ms.

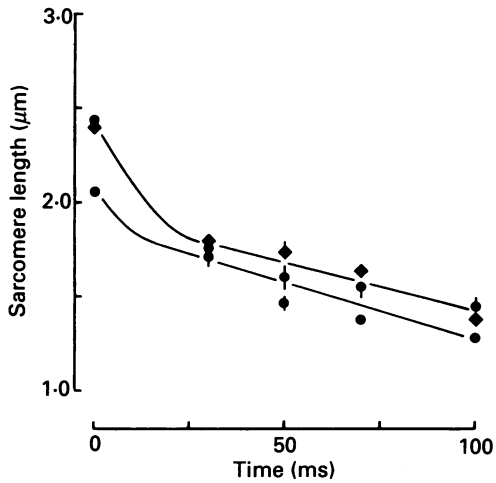

Fig. 5. Active shortening of myofibrils in the medium containing KCl concentrations above 100 mM. Shortening was initiated by adding $CaCl_2$ (final concentration 0·5 mM) at time = 0 to myofibrils which had been pre-incubated with 2 mM-Mg-ATP and 50 μM-EGTA for 1 s. Curves were drawn by eye. Symbols: ◆, 100 mM-KCl; ●, 150 mM-KCl. Error bars represent ± 1 S.E.M.

Figure 5 illustrates time courses of shortening at high ionic strengths (KCl concentrations > 100 mM), initiated by an increase in calcium concentration. At 30 ms after addition of $CaCl_2$ to stretched myofibrils (initial sarcomere length, 2·4 μm) in 100 mM-KCl, sarcomere length was already 1·8 μm and then a slower shortening followed. Most of the myofibrils showed the contraction bands at 100 ms and rapidly changed into amorphous aggregates after 150 ms. In 150 mM-KCl, similar rapid shortening occurred for the initial 30 ms period, after which the contraction bands were gradually formed but amorphous aggregates were not formed to any appreciable extent within a few seconds.

Taken together these results show that the initial phase of shortening is very rapid, the average shortening velocity $\geqslant 10\ \mu m\ s^{-1}$ (half-sarcomere, h.s.)$^{-1}$, which is comparable to the maximum shortening velocity (V_{max}) values reported for rabbit psoas muscle (4·4 muscle lengths s^{-1} at 15 °C, Moss, 1986) as well as other mammalian muscles (6–8 muscle lengths s^{-1} at 20–25 °C, Ranatunga, 1982; see also pp. 52–55, Woledge *et al.* 1985). It must be mentioned that shortening of myofibrils prepared from the muscles soaked in 50% (w/w) glycerol at −20 °C was only half as fast as that of those prepared as described in Methods.

Comparing the results in different KCl concentrations, one notices that both the

rapid and slow phase of shortening are affected by ionic strength. In higher KCl concentrations, initial shortening velocity is faster ($> 12\ \mu m\ s^{-1}$ (h.s.)$^{-1}$ in 150 mM-KCl *vs.* $10\ \mu m\ s^{-1}$ (h.s.)$^{-1}$ in 25 mM-KCl) whereas the slowing of shortening occurs at a longer sarcomere length (1·7–1·8 μm in KCl concentrations > 100 mM *vs.*

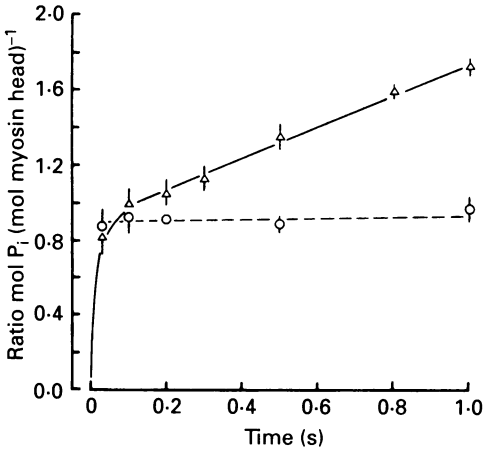

Fig. 6. Time courses of P_i formation following addition of Mg-ATP at time = 0 to myofibrils in the absence of calcium ions. EGTA (1 mM) was added as described in Fig. 3. Each point shows the mean ± 1 S.E.M. of five to ten measurements pooled for myofibrils of different sarcomere lengths. Regression lines were calculated on the basis of all the individual points for the P_i level (Y mol mol^{-1}) as a function of time (X s), $Y = a + b\,X$, where a and b are the estimates of initial burst and steady-state rate ($-Ca^{2+}$) respectively (see Table 2). Symbols: △, 25 mM-KCl ($Y = 0{\cdot}90 + 0{\cdot}81\,X$); ○, 150 mM-KCl ($Y = 0{\cdot}89 + 0{\cdot}066\,X$).

1·4–1·5 μm in 25 mM-KCl). As sarcomere length becomes shorter than 2·1 μm, the thin filaments overlap each other, which may increase the passive resistance to shortening. Both shortening velocity of single fibres under light load (Gordon *et al.* 1966) and tension in chemically skinned fibres (Allen & Moss, 1987) decrease at shorter sarcomere lengths. At higher ionic strengths, probably fewer cross-bridges may participate in force generation (see Discussion) and for this reason, shortening would become slow at a longer sarcomere length as the cross-over region of the thin filaments increases.

ATP hydrolysis by myofibrils

ATP hydrolysis in the absence of calcium ions

The kinetics of ATP hydrolysis by myofibrils of different sarcomere lengths in the presence of 1 mM-EGTA were first examined separately, but no systematic difference was found between them. Thus, the data points shown in Fig. 6 are those of averaged results for myofibrils of different sarcomere lengths.

In 25 mM-KCl, there was an initial phosphate burst of 0·9 mol (mol myosin heads)$^{-1}$ on addition of ATP, which was followed by steady ATP hydrolysis. The burst was completed in the first 30–50 ms after addition of ATP. It follows that most

of the cross-bridges bind and cleave ATP very rapidly ($> 40\ s^{-1}$ if approximated as an exponential process) and then release P_i much more slowly. This is consistent with the result obtained for chemically skinned psoas fibres using the laser-flash and quench method with caged ATP (Ferenczi *et al.* 1984). A high rate of steady ATP hydrolysis (0·8–0·9 s^{-1}) can be ascribed to the low ionic strength, since at high ionic strengths the rate decreased below 0·1 s^{-1} without significant change in the magnitude of phosphate burst.

These results as well as those given below are summarized in Table 2.

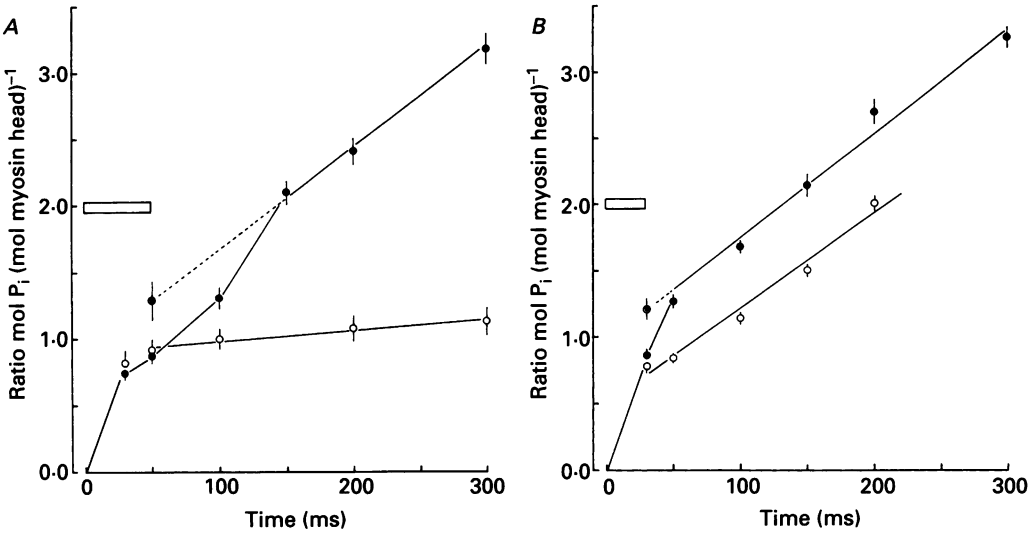

Fig. 7. Time courses of P_i formation during active shortening of myofibrils in 25 mM-KCl. shortening was induced as described in Fig. 4 (horizontal bars, rapid shortening phases). Each point is the mean ± 1 S.E.M. of at least three measurements in two to four independent experiments. Regression lines, $Y = a + bX$, were calculated using data for times given below, where a and b refer to estimated ATP hydrolysis at the time of onset of slow shortening and steady-state rate respectively. ⊙, the estimated ATP hydrolysis levels ± estimated standard deviation. *A*: ●, stretched myofibrils ($Y = 1{\cdot}29 + 7{\cdot}70\,X$, fitted to the data at times greater than 100 ms; $X = 0$ at 50 ms); ○, ATP hydrolysis in the presence of 1 mM-EGTA (the same data as for 25 mM-KCl in Fig. 6). *B*: ●, non-stretched myofibrils ($Y = 1{\cdot}10 + 8{\cdot}23\,X$, fitted to the data at times greater than 30 ms; $X = 0$ at 30 ms). ○, pre-contracted myofibrils ($Y = 0{\cdot}49 + 7{\cdot}14\,X$, fitted to the data at times greater than 0 ms; $X = 0$ at 0 ms).

ATP hydrolysis during active shortening at low ionic strength

Time courses of ATP hydrolysis in 25 mM-KCl are compared for stretched, non-stretched and pre-contracted myofibrils in Fig. 7. For stretched myofibrils (Fig. 7*A*), the P_i level for the first 50 ms, 0·87 ± 0·058 mol (mol myosin heads)$^{-1}$ (mean ± S.E.M., $n = 4$) during which sarcomeres shortened below 1·6 μm, was not significantly different from that observed in the absence of calcium ions, 0·92 ± 0·075 mol mol^{-1} ($n = 7$; $P > 0{\cdot}6$). As the contraction bands were formed and compressed, P_i increased

TABLE 2. Summary of results for ATP hydrolysis

KCl (mM)	25	25	100	150	150
Sarcomere length (μm)	2·4	2·0	2·4	2·4	2·0
Initial burst (mol mol^{-1})	0·901 ± 0·078		0·891 ± 0·049		
Steady-state $-Ca^{2+}$	0·810 ± 0·438		0·066 ± 0·111		
rate (s^{-1}) $+Ca^{2+}$	7·700 ± 0·861	8·320 ± 0·479	2·804 ± 0·414	1·605 ± 0·463	1·709 ± 0·599
ATP hydrolysis during rapid shortening (mol mol^{-1})	−0·050 ± 0·115	0·038 ± 0·096	−0·030 ± 0·112	−0·016 ± 0·089	0·014 ± 0·093
Delayed ATP hydrolysis (mol mol^{-1})	0·419 ± 0·190	0·238 ± 0·099	0·313 ± 0·104	0·169 ± 0·091	−0·020 ± 0·093

All data are given ± estimated standard deviation. Initial burst and steady-state rate ($-Ca^{2+}$) are the intercept and slope values, respectively, of the regression lines shown in Fig. 6. Steady-state rates ($+Ca^{2+}$) are the slopes of the regression lines in Figs 7 and 8. ATP hydrolysis during rapid shortening is the difference between P_i levels with and without Ca^{2+}; for 25 mM-KCl these values are from Fig. 7 where for sarcomere length 2·0 μm the values at 30 ms were used, and for sarcomere length 2·4 μm the values at 50 ms were used. For 100 and 150 mM-KCl, the ATP hydrolysis during rapid shortening is the difference between the values at 30 and 0 ms after the addition of $CaCl_2$ in Fig. 8. None of these values is significantly different from zero. See Table 3 for delayed ATP hydrolysis.

TABLE 3. Effects of initial sarcomere length and ionic strength on delayed ATP hydrolysis

KCl (mM)	25	25	100	150	150
Sarcomere length (μm)	2·4	2·0	2·4	2·4	2·0
Observed ATP hydrolysis (mol mol^{-1})	0·870 ± 0·087 (4)	0·860 ± 0·054 (5)	0·924 ± 0·079 (7)	1·035 ± 0·49 (8)	0·884 ± 0·071 (10)
Estimated ATP hydrolysis (mol mol^{-1})	1·289 ± 0·169 (11)	1·098 ± 0·079 (21)	1·237 ± 0·067 (42)	1·204 ± 0·076 (33)	0·864 ± 0·061 (42)
Delayed ATP hydrolysis (mol mol^{-1})	0·419 ± 0·190 (5·5)	0·238 ± 0·099 (14·5)	0·313 ± 0·104 (7·1)	0·169 ± 0·091 (11·6)	−0·020 ± 0·093 (12·6)
Student's t test values	1·98	2·40	3·00	1·87	0·21
Significance levels	< 0·05	< 0·025	< 0·01	< 0·05	< 0·4

Observed ATP hydrolysis values are means (± S.E.M. number of observations in parentheses) and the estimated ATP psoas muscle are calculated from regression lines as described below (± estimated standard deviation, degrees of freedom in parentheses). The delayed ATP hydrolysis is the difference between the observed and estimated values (± estimated standard deviation, degrees of freedom in parentheses). See Methods for estimation of the number of degrees of freedom of the difference. Significance levels are for Student's one-tailed t test. For sarcomere length 2·4 μm in 25 mM-KCl the observed ATP hydrolysis value is that shown in Fig. 7 at 50 ms, and the estimated value is that calculated for 50 ms from the regression based on data for times greater than 150 ms. For sarcomere length 2·0 μm the observed and estimated values are those at 30 ms; the latter was calculated from the regression based on data for times greater than 30 ms. In 100 and 150 mM-KCl the observed ATP hydrolysis is that shown in Fig. 8 at 30 ms, and the estimated value is that calculated for 30 ms from the regression based on data for times greater than 30 ms.

progressively faster for the next 100 ms or so. The rate of P_i formation then decreased to $7{\cdot}7 \pm 0{\cdot}9\ s^{-1}$, which compares with that observed for pre-contracted myofibrils, $7{\cdot}2 \pm 0{\cdot}7\ s^{-1}$. A similar diphasic ATP hydrolysis following the initial phosphate burst was recently observed for shortening myofibrils by Harada, Sakurada, Aoki, Thomas & Yanagida (1990).

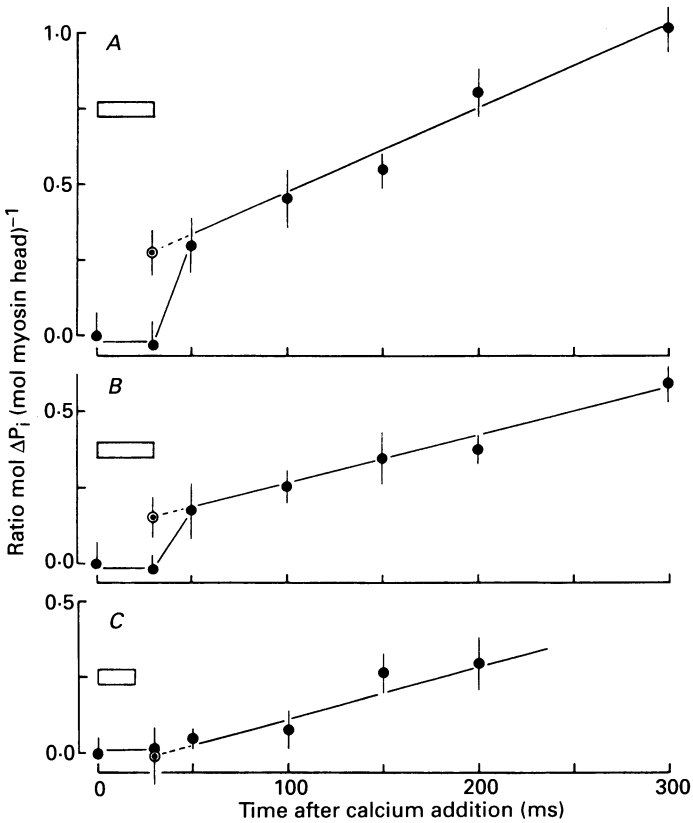

Fig. 8. Time courses of P_i increase during active shortening of myofibrils at high ionic strengths. At time = 0 (1 s after addition of Mg-ATP), $CaCl_2$ was added to induce shortening as described in Fig. 5. The ordinate is the increment of P_i level from the level before addition of $CaCl_2$ ($P_{i,o}$). Horizontal bars indicate approximate duration of the rapid shortening phase. Each point shows the mean $\pm$ 1 S.E.M. of at least five measurements in five to seven independent experiments. Regression lines, $Y = a + bX$, were calculated using data for times greater than 30 ms, i.e. $X = 0$ at 30 ms; a and b refer to the estimated ATP hydrolysis and steady-state rate as in Fig. 7 (see Table 3). $\odot$, estimated ATP hydrolysis levels $\pm$ estimated standard deviation. *A*, stretched myofibrils in 100 mM-KCl ($P_{i,o}$ $0{\cdot}95 \pm 0{\cdot}08$ mol (mol myosin head)$^{-1}$), $Y = 1{\cdot}24 + 2{\cdot}80\ X$). *B*, stretched myofibrils in 150 mM-KCl ($P_{i,o}$, $1{\cdot}05 \pm 0{\cdot}07$ mol mol^{-1}), $Y = 1{\cdot}20 + 1{\cdot}61\ X$. *C*, non-stretched myofibrils in 150 mM-KCl ($P_{i,o}$, $0{\cdot}87 \pm 0{\cdot}08$ mol mol^{-1}), $Y = 0{\cdot}86 + 1{\cdot}71\ X$.

The kinetics of ATP hydrolysis by non-stretched myofibrils are apparently less complicated than for stretched myofibrils (Fig. 7*B*). There was a rapid phase for the first 30–50 ms during which the heavy contraction bands were already dominant; the

P_i levels were $0{\cdot}86 \pm 0{\cdot}053$ mol mol^{-1} ($n = 5$) at 30 ms and $1{\cdot}27 \pm 0{\cdot}058$ mol mol^{-1} ($n = 5$) at 50 ms. It seems that the initial phosphate burst is immediately followed by the accelerated phase of ATP hydrolysis accompanying the formation and compression of the contraction bands. Then as amorphous aggregates were formed, the rate of ATP hydrolysis gradually settled down to $8{\cdot}2 \pm 0{\cdot}5$ s^{-1}, a similar value to that shown by pre-contracted myofibrils (see Table 2).

The accelerated ATP hydrolysis in the post-rapid shortening period is referred to as delayed ATP hydrolysis. Its magnitude can be estimated as the difference at the time of onset of slow shortening between the observed value and the least-squares estimate from the straight line fitted to the data points for the steady-state hydrolysis by linear regression (see Table 3). The magnitude thus estimated at 30 ms for non-stretched myofibrils was $0{\cdot}42 \pm 0{\cdot}19$ mol mol^{-1} and that estimated at 50 ms for stretched myofibrils was $0{\cdot}24 \pm 0{\cdot}10$ mol mol^{-1}. These are both significantly larger than zero as shown in Table 3.

ATP hydrolysis during active shortening at high ionic strength

Figure 8*A* shows ATP hydrolysis by stretched myofibrils triggered by increasing calcium ion concentration in 100 mM-KCl. The P_i level at 30 ms, by which time sarcomere length had rapidly shortened to 1·7 μm, was not significantly different from that before the increase in calcium ions ($P > 0{\cdot}8$; Table 2). Accompanying the slowing of shortening, there was a significant burst of ATP hydrolysis, $0{\cdot}31 \pm 0{\cdot}10$ mol mol^{-1} ($P < 0{\cdot}01$) as observed in 25 mM-KCl (delayed ATP hydrolysis), followed by a steady slow hydrolysis. Figure 8*B* shows a similar result in 150 mM-KCl, indicating no significant increase in P_i level for the first 30 ms ($P > 0{\cdot}8$) followed by a small but significant extent of delayed ATP hydrolysis, $0{\cdot}17 \pm 0{\cdot}09$ mol mol^{-1} ($P < 0{\cdot}05$). For non-stretched myofibrils (Fig. 8*C*), however, the slow shortening phase was simply accompanied by a steady slow ATP hydrolysis, and no delayed ATP hydrolysis was observed to any significant extent ($P > 0{\cdot}4$). These results together with those obtained in 25 mM-KCl suggest that the delayed ATP hydrolysis diminishes with a decrease of filament sliding distance as well as with an increase in ionic strength. This is in contrast with the steady-state rate of ATP hydrolysis, which is independent of initial sarcomere length and becomes greater at a lower ionic strength (Table 2).

DISCUSSION

The major result of these experiments is that during rapid shortening with zero load, there is no significant ATP turnover by cross-bridges for distances of filament sliding of 1 μm. For example, the upper 95% confidence limit of the ATP turnover for the first 30 ms after addition of calcium ions is 0·12 mol (mol myosin head) for pooled results in KCl concentrations $\geqslant$ 100 mM. It follows that either ADP or ADP and P_i remain bound to cross-bridges during the rapid shortening, since, if the cross-bridges had released the products, they would have bound new ATP molecules and cleaved them, rapidly increasing the P_i level. When shortening is slowed at shorter sarcomere lengths, there is a transient acceleration of ATP hydrolysis (delayed ATP hydrolysis), which is then followed by the steady-state hydrolysis. The magnitude of

delayed ATP hydrolysis decreases with the distance of shortening or filament sliding but increases with the decrease in ionic strength (Table 2).

Comparison with previous work on myofibrils and whole muscles

Myofibrils have long been used for kinetic analysis of ATP hydrolysis by actomyosin in a more organized state than that in solution. It was a major breakthrough in our understanding of the mechanochemical coupling that Yanagida, Arata & Oosawa (1985) measured the shortening velocity of fluorescently labelled actin filaments of crab myofibrils with a light microscope and the rate of accompanying ATP hydrolysis. Their results indicate that the average sliding distance of the actin filament is > 60 nm per one ATP cycle at zero load, much larger than the working stroke of a cross-bridge ($\leqslant$ 15 nm, see Ford, Huxley & Simmons, 1977).

The present work uses myofibrils prepared from rabbit psoas muscle to follow up the experiments of Yanagida *et al.* (1985). Given the differences in experimental conditions, our result is consistent with their observation. In addition, this work is the first to demonstrate, using myofibrils, that there is a delay ATP hydrolysis immediately after the rapid shortening phase is over.

This modulation of kinetics of ATP hydrolysis by shortening myofibrils can be compared to the energetic behaviour of rapidly shortening muscle. Following the earlier work by Kushmerick & Davies (1969), Rall *et al.* (1976) and Homsher *et al.* (1981) showed a production of heat during the rapid shortening phase which is not due to ATP hydrolysis. Immediately after the shortening, this energy imbalance is compensated by a post-shortening burst of ATP hydrolysis, which is more than that required to explain the concomitant heat production. In other words, although the ATP turnover rate is increased for the shortening and post-shortening periods together, it is not increased in phase with shortening itself. The delayed ATP hydrolysis (following 'unexplained' energy production) has been also observed in rapid shortening without preceding isometric contractions (Rall *et al.* 1976). This is what is demonstrated here with myofibrils in a temporally more precise way than for whole muscles.

Delayed ATP hydrolysis and energetics of rapidly shortening muscle

Thus, the delayed ATP hydrolysis is a genuine property of the contractile machinery of muscle manifested at zero- or near zero-load. Therefore, it is a crucial test of any hypothesis for the energetics of the rapidly shortening muscle whether it can adequately explain the delayed ATP hydrolysis or not.

It is well known that isometric tension in skinned fibres increases with the decrease in ionic strength. So does the binding strength of myosin head to actin in the presence of ATP (Greene, Sellers, Eisenberg & Adelstein, 1983; Katoh & Morita, 1984). These facts indicate that more cross-bridges participate in force generation at a lower ionic strength. It seems plausible, therefore, to take the magnitude of the delayed ATP hydrolysis by myofibrils as a measure of the proportion of cross-bridges (f) which have generated force during the rapid shortening phase. The f values at high ionic strengths ($\sim$ 0·2 in KCl concentrations > 100 mM) are indeed in good agreement with those for shortening muscle estimated by dynamic stiffness measurements

(Ford, Huxley & Simmons, 1985; Brenner & Eisenberg, 1986). With this important clue in hand, here we give an explanation of the energetics of rapidly shortening muscle on the basis of unique kinetic/energetic properties of the cross-bridge (Kodama, 1985).

There have been a number of reports suggesting that a myosin intermediate with bound ADP and P_i (M–ADP–P_i) in the ATP cycle is the cross-bridge state that generates force by interacting with actin filaments (Nagano & Yanagida, 1984; Goldman, 1987; Molloy, Kyrtatas, Sparrow & White, 1987). Calorimetric studies (Kodama, 1985) indicate that this state is at a high energy (enthalpy) level due to protein dehydration and a large amount of heat is produced on slow P_i dissociation. A part (~ 50 kJ mol^{-1}) of the heat comes from internal reaction of the protein. The rest is ascribed to the interaction of buffer with protons produced by ionization of the phosphate dissociated, amounting to 40 kJ mol^{-1} in a solution similar to the sarcoplasm in composition. The enthalpy change for the overall cycle (ATP hydrolysis) is -60 kJ mol^{-1} inclusive of the heat from buffer–proton interaction so that the intermediate steps other than the P_i dissociation together absorb heat as much as 30 kJ mol^{-1}.

It is also known that P_i dissociation is extremely slow in the absence of actin, but its rate constant does not change (0·031–0·035 s^{-1}) in the temperature range between 5 and 23 °C (Kodama, 1981), that is to say the apparent activation energy is effectively nil. This suggests that the rate-limiting step in this reaction is an energy-controlled process in which the rate is proportional to the amount of energy change per unit time but independent of temperature (T. Kodama, unpublished observation).

These unique properties of the cross-bridge state with bound ADP and P_i could account for the fact that at zero load, a single cross-bridge can drive actin filaments to slide over a distance much longer than the working stroke of a cross-bridge during one ATP cycle (Yanagida *et al.* 1985; Harada *et al.* 1990).

Explanation of the delayed ATP hydrolysis

During rapid shortening of myofibrils, an actin filament is driven to slide past cross-bridges at $V = 10$ μm s^{-1}. If the maximum distance that a cross-bridge remains attached to a given actin monomer is 15 nm (Ford *et al.* 1977), the maximum duration of attachment is equal to 15 nm $V^{-1} = 1{\cdot}5$ ms. This duration is too short for P_i to dissociate from the cross-bridges, but it would be long enough to allow a certain distortion of protein conformation to occur at the actin–myosin interface if one takes into account that the second-order rate constant for association of actin with myosin is $> 10^6$ M^{-1} s^{-1} (Hibberd & Tretham, 1986) and that the overall average concentration of actin in myofibril lattice is 0·7 mM (Yates & Greaser, 1983).

The conformational distortion thus induced could be a 'push' of the actin filament. When detachment then occurs rapidly, the filament would be translated by a net decrease in the energy level of protein associated with partial hydration of the myosin surface. In this way, a cross-bridge with bound ADP and P_i could change over from one actin monomer after another and 'push' them in turn by dissipating a fraction of the stored energy. Thus, 'unexplained' energy is produced while the actin filament is driven for a long distance during one ATP cycle, since no hydrolysis

products would be released until all of the stored energy is used up. Its magnitude should depend on the proportion of cross-bridges generating force and the distance of filament sliding or shortening.

When the force opposing filament sliding suddenly increases, the cross-bridges of lower energy levels due to participation in force generation at zero load would rapidly dissociate P_i and ADP and then enter the next ATP cycle in preference to others. Not much heat would be produced by these cross-bridges, because the heat produced by the proton–buffer interaction on the P_i dissociation is cancelled out by the heat absorption accompanying ADP dissociation and subsequent binding and cleavage of new ATP molecules together. This would be the delayed ATP hydrolysis without heat production in the post-shortening period.

This hypothesis is clearly distinct from earlier ones within the framework of the classic cross-bridge theory (Huxley, 1957; Huxley, 1969; Huxley & Simmons, 1971) which tacitly assumes that one ATP cycle is tightly coupled to one power-stroke (mechanical) cycle. Rall *et al.* (1976) proposed that cross-bridge detachment from actin may occur before product dissociation, resulting in temporal dissociation of energy liberation and ATP hydrolysis during rapid shortening. Homsher (1987) suggested that during rapid shortening, some cross-bridges would be forcedly detached (torn) from the thin filament after releasing P_i so that the cross-bridge with bound ADP would be accumulated; upon the cessation of shortening, dissociation of ADP would rapidly takes place, followed by a burst of ATP cleavage.

To test these hypotheses, it must be determined which chemical states of cross-bridges actually occurs during mechanochemical coupling, in particular whether or not P_i remains bound to cross-bridges during rapid shortening. It is needed to monitor an increment of free P_i concentration in solutions containing a contractile system with high chemical resolution in both absolute (< 100 nM) and relative ($< 1\%$) terms.

Support for this project was provided by Grants-in-Aid for Scientific Research on Priority Areas of 'Molecular Mechanism of Biological Sliding Movements' from the Ministry of Education, Science and Culture of Japan. We thank Professor Y. Umazume for his interest and constant support, and Professor T. Yanagida for discussion on many aspects of mechanochemical coupling.

REFERENCES

ALLEN, J. D. & MOSS, R. L. (1987). Factors influencing the ascending limb of the sarcomere length–tension relationship in rabbit skinned muscle fibres. *Journal of Physiology* **390**, 119–136.

ASPIN, A. A. (1949). Tables for use in comparisons whose accuracy involves two variances separately estimated. *Biometrika* **36**, 290–296.

BRENNER, B. & EISENBERG, E. (1986). Rate of force generation in muscle: Correlation with actomyosin ATPase activity in solution. *Proceedings of National Academy of Sciences of the USA* **83**, 3542–3546.

EDMAN, K. A. P. (1979). The velocity of unloaded shortening and its relation to sarcomere length and isometric force in vertebrate muscle fibres. *Journal of Physiology* **291**, 143–159.

FERENCZI, M. A., HOMSHER, E. & TRENTHAM, D. R. (1984). The kinetics of magnesium adenosine triphosphate cleavage in skinned muscle fibres of the rabbit. *Journal of Physiology* **352**, 575–599.

FORD, L. E., HUXLEY, A. F. & SIMMONS, R. M. (1977). Tension responses to sudden length change in stimulated frog muscle fibres near slack length. *Journal of Physiology* **269**, 441–515.

FORD, L. E., HUXLEY, A. F. & SIMMONS, R. M. (1985). Tension transients during steady shortening of frog muscle fibres. *Journal of Physiology* **361**, 131–150.

GOLDMAN, Y. E. (1987). Kinetics of the actomyosin ATPase in muscle fibers. *Annual Review of Physiology* **49**, 637–654.

GORDON, A. M., HUXLEY, A. F. & JULIAN, F. J. (1966). The variation in isometric tension with sarcomere length in vertebrate muscle fibres. *Journal of Physiology* **184**, 170–192.

GORNALL, A. G., BARDWILL, C. J. & DAVID, M. M. (1949). Determination of serum proteins by means of the biuret reaction. *Journal of Biological Chemistry* **177**, 751–766.

GREENE, L. E., SELLERS, J., EISENBERG, E. & ADELSTEIN, R. S. (1983). Binding of gizzard smooth muscle myosin subfragment 1 to actin in the presence and absence of adenosine 5′-triphosphate. *Biochemistry* **22**, 530–535.

HANSON, J. & HUXLEY, H. E. (1955). The structural basis of contraction in striated muscle. *Symposium of the Society for Experimental Biology* **9**, 228–264.

HARADA, Y., SAKURADA, K., AOKI, T., THOMAS, D. D. & YANAGIDA, T. (1990). Mechanochemical coupling in actomyosin energy transduction studied by in vitro movement assay. *Journal of Molecular Biology* **216**, 49–68.

HIBBERD, M. G. & TRENTHAM, D. R. (1986). Relationships between chemical and mechanical events during muscular contraction. *Annual Review of Biophysics and Biophysical Chemistry* **15**, 119–161.

HOMSHER, E. (1987). Muscle enthalpy production and its relationship to actomyosin ATPase. *Annual Review of Physiology* **49**, 673–690.

HOMSHER, E., IRVING, M. & WALLNER, A. (1981). High-energy phosphate metabolism and energy liberation associated with rapid shortening in frog skeletal muscle. *Journal of Physiology* **321**, 423–436.

HOMSHER, E., YAMADA, T., WALLNER, A. & TSAI, J. (1984). Energy balance studies in frog skeletal muscles shortening at one-half maximal velocity. *Journal of General Physiology* **84**, 347–359.

HUXLEY, A. F. (1957). Muscle structure and theories of contraction. *Progress in Biophysics and Biophysical Chemistry* **7**, 255–318.

HUXLEY, A. F. & SIMMONS, R. M. (1971). Proposed mechanism of force generation in striated muscle. *Nature* **233**, 533–538.

HUXLEY, H. E. (1969). The mechanism of muscular contraction. *Science* **164**, 1356–1366.

KANAZAWA, T., SAITO, M. & TONOMURA, Y. (1970). Formation and decomposition of a phosphorylated intermediate in the reaction of Na^+–K^+ dependent ATPase. *Journal of Biochemistry* **67**, 693–711.

KATOH, T. & MORITA, F. (1984). Interaction between myosin and F-actin. Actin-binding sites on subfragment-1. *Journal of Biochemistry* **96**, 1223–1230.

KODAMA, T. (1981). Reaction heats and heat capacity changes for intermediate steps of the ATP hydrolysis catalyzed by myosin subfragment 1. *Journal of Biological Chemistry* **256**, 2928–2933.

KODAMA, T. (1985). Thermodynamic analysis of muscle ATPase mechanisms. *Physiological Reviews* **65**, 467–551.

KODAMA, T., FUKUI, K. & KOMETANI, K. (1986). The initial phosphate burst in ATP hydrolysis by myosin and subfragment-1 as studied by a modified Malachite Green method for determination of inorganic phosphate. *Journal of Biochemistry* **99**, 1465–1472.

KUSHMERICK, K. M. & DAVIES, R. E. (1969). The chemical energetics of muscle contraction. II. The chemistry, efficiency and power of maximally working sartorius muscles. *Proceedings of the Royal Society* B **174**, 315–350.

LANZETTA, P. A., ALVAREZ, L. J., REINACH, P. S. & CANDIA, O. A. (1979). An improved assay for nanomole amounts of inorganic phosphate. *Analytical Biochemistry* **100**, 95–97.

MOLLOY, J. E., KYRTATAS, V., SPARROW, J. C. & WHITE, D. C. S. (1987). Kinetics of flight muscles from insects with different wingbeat frequencies. *Nature* **328**, 449–451.

MOSS, R. L. (1986). Effects on shortening velocity of rabbit skeletal muscle due to variation in the level of thin filament activation. *Journal of Physiology* **377**, 487–505.

NAGANO, H. & YANAGIDA, T. (1984). Predominant attached state of myosin cross-bridges during contraction and relaxation at low ionic strength. *Journal of Molecular Biology* **177**, 769–785.

NAKATUKA, T., NAKAMURA, N. & SANO, T. (1988). Application of hydrogen ion sensitive field effective transistor to the kinetic study of fast reaction in solution. *Bulletin of Chemical Society of Japan* **61**, 799–802.

OHNO, T. & KODAMA, T. (1989). ATP hydrolysis by shortening myofibrils. In *Muscle Energetics*, ed. PAUL, R. J., ELZINGA, G. & YAMADA, K., pp. 69–73. Alan R. Liss Inc., New York.

PAGE, S. & HUXLEY, H. E. (1963). Filament lengths in striated muscle. *Journal of Cell Biology* **19**, 369–390.

RALL, J., HOMSHER, E., WALLNER, A. & MOMMAERTS, W. F. H. M. (1976). A temporal dissociation of energy liberation and high energy phosphate splitting during shortening in frog skeletal muscle. *Journal of General Physiology* **68**, 13–27.

RANATUNGA, K. W. (1982). Temperature-dependence of shortening velocity and isometric tension development in rat skeletal muscle. *Journal of Physiology* **329**, 465–483.

WOLEDGE, R. C., CURTIN, N. A. & HOMSHER, E. (1985). *Energetic Aspects of Muscle Contraction*. Academic Press, New York.

YANAGIDA, T., ARATA, T. & OOSAWA, F. (1985). Sliding distance of actin filament induced by a myosin crossbridge during one ATP hydrolysis cycle. *Nature* **316**, 366–369.

YASUDA, H. & STANNETT, V. (1975). Permeability coefficients. In *Polymer Handbook*, ed. BRANDRUP, J. & IMMERGUT, E. H., pp. III 229–III 240. John Wiley, New York.

YATES, L. D. & GREASER, M. L. (1983). Quantitative determination of myosin and actin in rabbit skeletal muscle. *Journal of Molecular Biology* **168**, 123–141.